 cmes, vol.5, no.6, pp.541-562, 2004

Directly Derived Non-Hyper-Singular Boundary Integral Equations for Acoustic Problems, and Their Solution through Petrov-Galerkin Schemes

Z.Y. Qian[1], Z.D. Han[1], and S.N. Atluri[1]

Abstract: Novel non-hyper-singular [i.e., only strongly-singular] boundary-integral-equations for the gradients of the acoustic velocity potential, involving only $O(r^{-2})$ singularities at the surface of a 3-D body, are derived, for solving problems of acoustics governed by the Helmholtz differential equation. The gradients of the fundamental solution to the Helmholtz differential equation for the velocity potential, are used in this derivation. Several basic identities governing the fundamental solution to the Helmholtz differential equation for velocity potential, are also derived. Using these basic identities, the strongly singular integral equations for the potential and its gradients [denoted here as ϕ-BIE, and q-BIE, respectively], are rendered to be only weakly-singular [i.e., possessing singularities of $O(r^{-1})$ at the surface of a 3-D body]. These weakly-singular equations are denoted as R-ϕ-BIE, and R-q-BIE, respectively. General Petrov-Galerkin weak-solutions of R-ϕ-BIE, and R-q-BIE are discussed; and special cases of collocation-based boundary-element numerical approaches [denoted as BEM-R-ϕ-BIE, and BEM-R-q-BIE], as well as Symmetric Galerkin Boundary Element approaches [denoted as SGBEM-R-ϕ-BIE and SGBEM-R-q-BIE, respectively] are also presented. The superior accuracy and efficiency of the SGBEM-R-ϕ-BIE and SGBEM-R-q-BIE are illustrated, through examples involving acoustic radiation as well as scattering from 3-D bodies possessing smooth surfaces, as well as surfaces with sharp corners.

keyword: Boundary integral equations, hyper-singularity, Petrov-Galerkin

1 Introduction

The difficulties in dealing with hyper-singular integrals, and the nonuniqueness, are two of the well known drawbacks of the existing boundary integral equation (BIE) methods for solving acoustic problems, even though the boundary integral equation method offers more advantages over other popular numerical methods such as the finite element method [Chien, Rajiyah, and Atluri (1990)]. In 1968, Schenck pointed out that the integral equation for potential mathematically failed to yield unique solutions to the exterior acoustic problem, and proposed a method labeled as CHIEF[Schenck (1968)], in which an over-determined system of equations at some characteristic frequencies was formed by combining the surface Helmholtz equation with the interior Helmholtz equation. The system of equations was analytically proved to provide a unique solution at the characteristic frequencies, to some extent. However, the method might fail to produce unique solutions, when the interior points used in the collocation of BIEs were located on a nodal surface of an interior standing wave. The nonuniqueness of solutions, at certain frequencies of the associated acoustic problem in the interior of the solid body, is actually a purely mathematical issue arising from the boundary integral formulation, without any physical significance. Meanwhile, Burton and Miller (1971) developed a combination of the surface Helmholtz integral equation for potential, and the integral equation for the normal derivative of potential at the surface, to circumvent the problem of nonuniqueness at characteristic frequencies. Their method was labeled as CHIE (Composite Helmholtz Integral Equation), or CONDOR (Composite Outward Normal Derivative Overlap Relation) by Reut [Reut (1985)]. The CHIE method is more straightforward, as compared to the CHIEF method; however, it introduces the hypersingular integrals, which are computationally costly. Moreover, in CHIE method, the accuracy of the integrations affects the results, and the conventional Gauss quadrature can not be used directly. Regularization techniques are commonly employed by the followers of the CHIE methodology, to improve the approach by reducing the problem to the one involving

[1] Center for Aerospace Research & Education, 5251 California Ave, #140, University of California, Irvine, CA92612, USA

$O(r^{-1})$ singular integrals near the point of singularity. Chien, Rajiyah, and Atluri (1990) employed some known identities of the fundamental solution from the associated interior Laplace problem, to regularize the hypersingular integrals. This concept was used by many successive researchers: Hwang (1997) reduced the singularity of the Helmholtz integral equation also by using some identities from the associated Laplace equation. However, the value of the equipotential inside the domain must be computed, because the source distribution for the equipotential surface from the potential theory was used to regularize the weak singularities. Yang (2000) also uses the identities of the fundamental solution of the Laplace problem, to efficiently solve the problem of acoustic scattering from a rigid body. Besides, Meyer, Bell, Zinn, and Stallybrass (1978) and Terai (1980) developed regularization techniques for planar elements. The regularized normal derivative equation [Wu, Seybert, and Wan (1991)] proposed by Wu *et al.* converged in the Cauchy principal value sense, rather than in the finite-part sense. The computation of tangential derivatives was required everywhere on the boundary. Another way commonly used in the literature is to develop the methods to directly evaluate the hypersingular integrals. Recently, to solve the intensive computation of double surface integral, Yan, Hung, and Zheng (2003) employed the concept of a discretized operator matrix to replace the evaluation of double surface integral with the evaluation of two discretized operator matrices. In summary, most of *regularization techniques* for evaluating the hyper-singular integrals in the acoustic BIEs arise from certain identities associated with the fundamental solution to the Laplace equations.

In the present paper, however, novel non-hyper-singular boundary integral equations are derived directly, for the gradients of the velocity potential. The acoustic potential gradients are related to the sound velocity in their physical meaning. The basic idea of using the gradients of the fundamental solution to the Helmholtz differential equation for velocity potential, as *vector test-functions* to write the weak-form of the original Helmholtz differential equation for potential, and thereby directly derive a *non-hyper-singular boundary integral equations for velocity potential gradients*, has its origins in [Okada, Rajiyah, and Atluri (1989a, b), Okada and Atluri (1994)], which use the displacement and velocity gradients to directly establish the numerically tractable displacement and displacement gradient boundary integral equations in elastic/plastic solid problems, and traction boundary integral equations [Han and Atluri (2003a)]. The current method can be shown to be fundamentally different from the regularized normal derivative equation by Wu *et al.* [Wu, Seybert, and Wan (1991)], which used tangential derivatives to reduce the singularity.

The boundary integral equations for the potential [labeled here as ϕ-BIE], and its gradient [labeled here as q-BIE], which are used as starting points in the present paper, are only strongly singular [$O(r^{-2})$]. The further regularization of these *strongly singular* ϕ-BIE, and q-BIE, to *only weakly singular* [$O(r^{-1})$] types, which are labeled here as R-ϕ-BIE, R-q-BIE, respectively, is achieved *by using certain basic identities of the fundamental solution of the Helmholtz differential equation for potential*. These basic identities, in their most general form, are also newly derived in this paper. These basic identities are derived from the most general scalar and vector weak-forms of the Helmholtz differential equation for potential, *governing the fundamental solution itself*. The boundary element methods [BEM] derived by simply collocating the regularized ϕ-BIE, and q-BIE, as developed in the present paper, are referred to as the BEM-R-ϕ-BIE, and BEM-R-q-BIE, respectively. In addition, in the present paper, we formulate general Petrov-Galerkin methods to solve the R-ϕ-BIE, and R-q-BIE, in their weak senses. By using the test functions in these Petrov-Galerkin schemes to be the energy-conjugates of the respective trial functions, we develop Symmetric Galerkin Boundary Element Methods (SGBEM) for solving R-ϕ-BIE, and R-q-BIE, respectively. We label these SGBEM as SGBEM-R-ϕ-BIE and SGBEM-R-q-BIE, respectively. These SGBEM-R-ϕ-BIE and SGBEM-R-q-BIE are totally different from the ones in [Chen, Hofstetter, and Mang (1997), Gray and Paulino (1997)]. In the present SGBEM-R-ϕ-BIE and SGBEM-R-q-BIE, C^0 continuity of ϕ and q over the boundary elements is sufficient for numerical implementation. Though the double surface integral may increase the numerical accuracy of the SGBEM, many fast SGBEM methods are proposed to speed up the computation of double surface integrals, including panel clustering methods, wavelet methods and so on [Aimi, Diligenti, Lunardini, and Salvadori (2003), Breuer, Steinbach, and Wendland (2002)].

As another recent extension of boundary element methods, meshless methods for solving BIEs have been

developed through the meshless local Petrov-Galerkin (MLPG) approaches [Han, and Atluri (2003b)]. The meshless method, as an alternative numerical approach to eliminate the well known drawbacks in the finite element and boundary element methods, has attracted much attention recently [Atluri, Han, and Shen (2003); Atluri, and Shen (2002a, b)]. These are also briefly discussed in the present paper.

2 The governing wave equation, and its fundamental solution

The propagation of acoustic waves through an unbounded homogeneous medium is described by the wave equation:

$$\nabla^2\phi(r,t) - \frac{1}{c^2}\frac{\partial^2\phi(r,t)}{\partial t^2} = 0 \tag{1}$$

where ∇^2 denotes the Laplacian operator, ϕ is the acoustic velocity potential at a point r at time t, and c is the speed of sound in the medium at the equilibrium state. For time-harmonic waves with a time factor $e^{-i\omega t}$, the Helmholtz differential equation for ϕ can be written as follows:

$$\nabla^2\phi + k^2\phi = 0 \tag{2}$$

where i is the imaginary unit, ω is the angular frequency of the acoustic wave, and $k = \omega/c$ is the wave number.

The acoustic pressure p and the velocity $\mathbf{u}$ of the fluid particles induced by the sound waves are determined through the velocity potential ϕ, as:

$$p = -\rho_0\frac{\partial\phi}{\partial t} \tag{3}$$

and

$$\mathbf{u} = \nabla\phi \tag{4}$$

where ∇ is the gradient operator, and ρ_0 denotes the density of the fluid at the equilibrium state. For time-harmonic waves, we have:

$$p = i\omega\rho_0\phi \tag{5}$$

The power-flux-density of sound waves is given by:

$$\mathbf{P} = p\mathbf{u} = p\nabla\phi \tag{6}$$

In general, the acoustic velocity potential can be represented as a sum of the incident potential and the scattered potential:

$$\phi = \phi^i + \phi^s \tag{7}$$

At the surface of a soft scatterer, the boundary condition is

$$\phi = 0 \tag{8}$$

At the surface of a hard scatterer, the boundary condition on the normal component of the particle velocity is

$$\mathbf{n}\cdot\nabla\phi = 0 \tag{9}$$

in which, $\mathbf{n}$ is the unit outward normal vector of the surface. Usually these two conditions are generally referred to, as the Dirichlet and the Neumann boundary conditions, respectively. Also, the scattered potential should satisfy the Sommerfeld radiation condition

$$\lim_{r\to\infty} r\left|\frac{\partial\phi^s}{\partial r} - ik\phi^s\right| = 0 \text{ in 3D} \tag{10}$$

The fundamental solution of the Helmholtz differential equation Eq. (2) at any field point $\boldsymbol{\xi}$ due to a point sound source at $\mathbf{x}$, is well known as the free-space Green's function $G_k(\mathbf{x},\boldsymbol{\xi})$, which is listed here for 2- and 3-D problems, respectively, as follows:

For a 2D problem, the Green's function is:

$$G_k(\mathbf{x},\boldsymbol{\xi}) = \frac{i}{4}H_0^{(1)}(kr) \tag{11a}$$

$$\frac{\partial G_k}{\partial r}(\mathbf{x},\boldsymbol{\xi}) = -\frac{i}{4}kH_1^{(1)}(kr) \tag{11b}$$

where $H_0^{(1)}(kr)$ denotes the Hankel function of the first kind, and r represents the distance between the field point $\boldsymbol{\xi}$ and the source point $\mathbf{x}$. For a 3D problem,

$$G_k(\mathbf{x},\boldsymbol{\xi}) = \frac{1}{4\pi r}e^{-ikr} \tag{11c}$$

$$\frac{\partial G_k}{\partial r}(\mathbf{x},\boldsymbol{\xi}) = \frac{e^{-ikr}}{4\pi r^2}(-ikr-1) \tag{11d}$$

in which $r = |\mathbf{x}-\boldsymbol{\xi}|$, and $r_{,i} \equiv \frac{\partial r}{\partial \xi_i} = -\frac{x_i-\xi_i}{r}$.

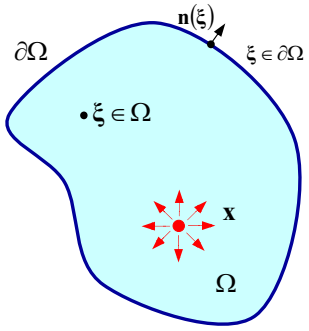

Figure 1 : A solution domain with source point $\mathbf{x}$

In the following sections, we use $\phi^*(\mathbf{x},\boldsymbol{\xi})$ to denote $G_k(\mathbf{x},\boldsymbol{\xi})$, without losing any generality. Consider a body of an infinite extent (Fig. 1), subject to a point sound source at a generic location $\mathbf{x}$. The fundamental solution is the sound field, denoted by $\phi^*(\mathbf{x},\boldsymbol{\xi})$, at any point $\boldsymbol{\xi}$ due to the point sound source, and is governed by the wave equation:

$$\nabla^2\phi^*(\mathbf{x},\boldsymbol{\xi}) + k^2\phi^*(\mathbf{x},\boldsymbol{\xi}) + \delta(\mathbf{x},\boldsymbol{\xi}) = 0 \tag{12a}$$

or

$$\phi^*_{,ii}(\mathbf{x},\boldsymbol{\xi}) + k^2\phi^*(\mathbf{x},\boldsymbol{\xi}) + \delta(\mathbf{x},\boldsymbol{\xi}) = 0 \tag{12b}$$

We also refer to Eq. (12) as the Helmholtz potential equation governing the fundamental solution.

3 Boundary integral equations for the velocity potential ϕ, and its gradient $\phi_{,k}$

3.1 *The current state-of-science for BIE in acoustics: Strongly singular ϕ and Hyper-singular $\phi_{,k}$*

Let $\overline{\phi}$ be the test function chosen to enforce the Helmholtz equation, Eq. (2), in terms of the trial function ϕ, in a weak form. The weak form of Helmholtz equation can then be written as:

$$\int_\Omega \left(\nabla^2\phi + k^2\phi\right)\overline{\phi}\,d\Omega = 0 \tag{13}$$

If we apply the divergence theorem once in Eq. (13), we obtain a "symmetric" weak form:

$$\int_{\partial\Omega} n_i\phi_{,i}\overline{\phi}\,dS - \int_\Omega \phi_{,i}\overline{\phi}_{,i}\,d\Omega + \int_\Omega k^2\phi\overline{\phi}\,d\Omega = 0 \tag{14}$$

Thus, in the "symmetric weak-form", both the trial function ϕ, as well as the test functions $\overline{\phi}$ are only required to be first-order differentiable. If we apply the divergence theorem twice in Eq. (13), we obtain:

$$\int_{\partial\Omega} n_i\phi_{,i}\overline{\phi}\,dS - \int_{\partial\Omega} n_i\phi\overline{\phi}_{,i}\,dS + \int_\Omega \phi\left(\overline{\phi}_{,ii} + k^2\overline{\phi}\right)d\Omega = 0 \tag{15}$$

We label Eq. (15) as the "unsymmetric weak-form". Now, the test functions $\overline{\phi}$ are required to be second-order differentiable, while ϕ is not required to be differentiable [Han and Atluri (2003a)] in Ω.

If we take the fundamental solution $\phi^*(\mathbf{x},\boldsymbol{\xi})$ to be the test function $\overline{\phi}$ in Eq. (15), and noting the property from Eq. (12), we have:

$$\begin{aligned}\phi(\mathbf{x}) &= \int_{\partial\Omega} n_i(\boldsymbol{\xi})\phi_{,i}(\boldsymbol{\xi})\phi^*(\mathbf{x},\boldsymbol{\xi})\,dS \\ &\quad - \int_{\partial\Omega} n_i(\boldsymbol{\xi})\phi(\boldsymbol{\xi})\phi^*_{,i}(\mathbf{x},\boldsymbol{\xi})\,dS \\ &\equiv \int_{\partial\Omega} q(\boldsymbol{\xi})\phi^*(\mathbf{x},\boldsymbol{\xi})\,dS - \int_{\partial\Omega}\phi(\boldsymbol{\xi})\Theta^*(\mathbf{x},\boldsymbol{\xi})\,dS\end{aligned} \tag{16}$$

where by definition,

$$q(\boldsymbol{\xi}) = \frac{\partial \phi(\boldsymbol{\xi})}{\partial n_\xi} = n_k(\boldsymbol{\xi})\,\phi_{,k}(\boldsymbol{\xi}) \quad \boldsymbol{\xi} \in \partial\Omega \tag{17}$$

and the kernel function,

$$\Theta^*(\mathbf{x},\boldsymbol{\xi}) = \frac{\partial \phi^*(\mathbf{x},\boldsymbol{\xi})}{\partial n_\xi} = n_k(\boldsymbol{\xi})\,\phi^*_{,k}(\mathbf{x},\boldsymbol{\xi}) \quad \boldsymbol{\xi} \in \partial\Omega \tag{18}$$

Thus, $q(\boldsymbol{\xi})$ is the potential gradient along the outward normal direction of the boundary surface.

Eq. (16) is the "traditional" BIE for ϕ, that is widely used in literature. We refer to Eq. (16), hereafter, as ϕ-BIE. The nonuniqueness of the solution of Eq. (16) arises because, this homogeneous equation has nontrivial solutions at some characteristic frequencies [Chien, Rajiyah, and Atluri (1990)]. As noted in the introduction, many researchers have investigated and expended substantial efforts in solving this problem of nonuniqueness.

If we differentiate Eq. (16) directly with respect to $\mathbf{x}_k$, we obtain the integral equations for potential gradients $\phi_{,k}(\mathbf{x})$ as:

$$\frac{\partial \phi(\mathbf{x})}{\partial x_k} = \int_{\partial\Omega} q(\boldsymbol{\xi}) \frac{\partial \phi^*(\mathbf{x},\boldsymbol{\xi})}{\partial x_k} dS - \int_{\partial\Omega} \phi(\boldsymbol{\xi}) \frac{\partial \Theta^*(\mathbf{x},\boldsymbol{\xi})}{\partial x_k} dS \tag{19}$$

The second term on the right hand side of Eq. (19) is hyper-singular, since $\frac{\partial \Theta^*(\mathbf{x},\boldsymbol{\xi})}{\partial x_k}$ is of order $O\left(r^{-3}\right)$ for a 3D problem. Eq. (19) is also the integral equations for the gradients of $\phi(\mathbf{x})$ that are widely used in the literature; and hence a wide body of literature is devoted to deal with the hyper-singularity in this equation.

3.2 *Presently proposed Non-Hyper-Singular BIE for* $\phi_{,k}$

On the other hand, the new method proposed in this paper starts *from writing a vector weak-form* [as opposed to a scalar weak-form] of the governing equation Eq. (13) by using the vector test functions $\overline{\phi}_{,k}$, as in [Okada, Rajiyah, and Atluri (1989a, 1989b)]:

$$\int_\Omega \left(\phi_{,ii} + k^2\phi\right)\overline{\phi}_{,k} d\Omega = 0 \;\; for \;\; k = 1,2,3 \tag{20}$$

After applying the divergence theorem three times in Eq. (20), we can write:

$$\int_{\partial\Omega} n_i \phi_{,i} \overline{\phi}_{,k} dS - \int_{\partial\Omega} n_k \phi_{,i} \overline{\phi}_{,i} dS + \int_{\partial\Omega} n_i \phi_{,k} \overline{\phi}_{,i} dS + \int_{\partial\Omega} k^2 n_k \phi \overline{\phi} dS - \int_\Omega \left(\overline{\phi}_{,ii} + k^2\overline{\phi}\right)\phi_{,k} d\Omega = 0 \tag{21}$$

Using the gradients of the fundamental solution, viz., $\phi^*_{,k}(\mathbf{x},\boldsymbol{\xi})$, as the test functions, and using the identity from Eq. (21), we obtain

$$\begin{aligned} -\phi_{,k}(\mathbf{x}) = &\int_{\partial\Omega} q(\boldsymbol{\xi})\,\phi^*_{,k}(\mathbf{x},\boldsymbol{\xi})\,dS \\ &- \int_{\partial\Omega} n_k(\boldsymbol{\xi})\,\phi_{,i}(\boldsymbol{\xi})\,\phi^*_{,i}(\mathbf{x},\boldsymbol{\xi})\,dS \\ &+ \int_{\partial\Omega} \phi_{,k}(\boldsymbol{\xi})\,\Theta^*(\mathbf{x},\boldsymbol{\xi})\,dS \\ &+ \int_{\partial\Omega} k^2 n_k(\boldsymbol{\xi})\,\phi(\boldsymbol{\xi})\,\phi^*(\mathbf{x},\boldsymbol{\xi})\,dS \end{aligned} \tag{22}$$

It should be noted that the integral equations for $\phi(\mathbf{x})$ [Eq. (16)], and $\phi_{,k}(\mathbf{x})$ [Eq. (22)], *are derived independently of each other*. The most interesting feature of the "directly derived" integral equations Eq. (22), for $\phi_{,k}(\mathbf{x})$, *is that they are non-hyper-singular, viz, the highest order singularity in the kernels appearing in Eq. (22) is only* $O\left(r^{-2}\right)$ *in a 3D problem*.

We define the surface tangential operator as

$$D_t = n_r e_{rst} \frac{\partial}{\partial \boldsymbol{\xi}_s} \tag{23}$$

in which e_{rst} is the permutation symbol. Then, we may rewrite Eq. (22) as:

$$\begin{aligned} -\phi_{,k}(\mathbf{x}) = &\int_{\partial\Omega} q(\boldsymbol{\xi})\,\phi^*_{,k}(\mathbf{x},\boldsymbol{\xi})\,dS \\ &+ \int_{\partial\Omega} D_t\phi(\boldsymbol{\xi})\,e_{ikt}\phi^*_{,i}(\mathbf{x},\boldsymbol{\xi})\,dS \\ &+ \int_{\partial\Omega} k^2 n_k(\boldsymbol{\xi})\,\phi(\boldsymbol{\xi})\,\phi^*(\mathbf{x},\boldsymbol{\xi})\,dS \end{aligned} \tag{24}$$

3.3 Some basic physical & mathematical properties of the fundamental solution ϕ^*, which permit simple and direct regularizations of the strongly singular BIEs for ϕ and $q(\phi_{,k})$

We write the weak form of Eq. (12), governing the fundamental solution, over the domain, using a constant c as the test function, and obtain

$$\int_\Omega \left[\nabla^2\phi^*(\mathbf{x},\boldsymbol{\xi})+k^2\phi^*(\mathbf{x},\boldsymbol{\xi})\right] c\,d\Omega + c = 0 \quad \text{at} \quad \mathbf{x}\in\Omega \tag{25a}$$

or

$$\int_\Omega \left[\phi^*_{,ii}(\mathbf{x},\boldsymbol{\xi})+k^2\phi^*(\mathbf{x},\boldsymbol{\xi})\right] d\Omega + 1 = 0 \quad \text{at} \quad \mathbf{x}\in\Omega \tag{25b}$$

or

$$\int_{\partial\Omega} n_i(\boldsymbol{\xi})\,\phi^*_{,i}(\mathbf{x},\boldsymbol{\xi})\,dS + \int_\Omega k^2\phi^*(\mathbf{x},\boldsymbol{\xi})\,d\Omega + 1 = 0 \quad \text{at} \quad \mathbf{x}\in\Omega \tag{25c}$$

Eq. (25c) is a "basic identity" of the fundamental solution$\phi^*(\mathbf{x},\boldsymbol{\xi})$. Now, consider an arbitrary function $\phi(\mathbf{x})$ in Ω as the test function, and once again write the weak form of Eq. (12), as

$$\int_\Omega \left[\nabla^2\phi^*(\mathbf{x},\boldsymbol{\xi})+k^2\phi^*(\mathbf{x},\boldsymbol{\xi})+\delta(\mathbf{x},\boldsymbol{\xi})\right]\phi(\mathbf{x})\,d\Omega = 0 \quad \text{at} \quad \mathbf{x}\in\Omega \tag{26a}$$

or

$$\int_\Omega \left[\phi^*_{,ii}(\mathbf{x},\boldsymbol{\xi})+k^2\phi^*(\mathbf{x},\boldsymbol{\xi})\right]\phi(\mathbf{x})\,d\Omega + \phi(\mathbf{x}) = 0 \quad \text{at} \quad \mathbf{x}\in\Omega \tag{26b}$$

or

$$\int_{\partial\Omega} \Theta^*(\mathbf{x},\boldsymbol{\xi})\,\phi(\mathbf{x})\,dS + \int_\Omega k^2\phi^*(\mathbf{x},\boldsymbol{\xi})\,\phi(\mathbf{x})\,d\Omega + \phi(\mathbf{x}) = 0 \quad \text{at} \quad \mathbf{x}\in\Omega \tag{26c}$$

Once the point $\mathbf{x}$ approaches a smooth boundary, i.e., $\mathbf{x}\in\partial\Omega$, the first term in Eq. (26c) can be written as

$$\lim_{\mathbf{x}\to\partial\Omega}\int_{\partial\Omega}\Theta^*(\mathbf{x},\boldsymbol{\xi})\,\phi(\mathbf{x})\,dS = \int_{\partial\Omega}^{CPV}\Theta^*(\mathbf{x},\boldsymbol{\xi})\,\phi(\mathbf{x})\,dS - \frac{1}{2}\phi(\mathbf{x}) \tag{27}$$

in which we introduce the notion of a Cauchy Principal Value (CPV) integral. The physical meaning of Eq. (27) can be understood by rewriting Eq. (25c) and (26c), respectively as:

$$\int_{\partial\Omega}^{CPV}\Theta^*(\mathbf{x},\boldsymbol{\xi})\,dS + \int_\Omega k^2\phi^*(\mathbf{x},\boldsymbol{\xi})\,d\Omega + \frac{1}{2} = 0 \quad \text{at} \quad \mathbf{x}\in\partial\Omega \tag{28a}$$

$$\int_{\partial\Omega}^{CPV}\Theta^*(\mathbf{x},\boldsymbol{\xi})\,\phi(\mathbf{x})\,dS + \int_\Omega k^2\phi^*(\mathbf{x},\boldsymbol{\xi})\,\phi(\mathbf{x})\,d\Omega + \frac{1}{2}\phi(\mathbf{x}) = 0 \quad \text{at} \quad \mathbf{x}\in\partial\Omega \tag{28b}$$

Eq. (28a) implies that only a half of the sound source at point $\mathbf{x}$ is applied to the domain Ω, when the point $\mathbf{x}$ approaches a smooth boundary, $\mathbf{x}\in\partial\Omega$. Eq. (28b) can be likewise interpreted physically.

We again consider another weak form of Eq. (12), by taking the vector test functions to be the gradients of an arbitrary function $\phi(\boldsymbol{\xi})$ in Ω, which are so chosen that they have constant values, as:

$$\phi_{,k}(\boldsymbol{\xi}) = \phi_{,k}(\mathbf{x}) \tag{29}$$

Then the weak form of Eq. (12) may be written as:

$$\int_\Omega \left[\phi^*_{,ii}(\mathbf{x},\boldsymbol{\xi})+k^2\phi^*(\mathbf{x},\boldsymbol{\xi})\right]\phi_{,k}(\boldsymbol{\xi})\,d\Omega + \phi_{,k}(\mathbf{x}) = 0 \tag{30}$$

After applying the divergence theorem, we can obtain from Eq. (30):

$$\int_{\partial\Omega}\Theta^*(\mathbf{x},\boldsymbol{\xi})\,\phi_{,k}(\mathbf{x})\,dS + \int_\Omega k^2\phi^*(\mathbf{x},\boldsymbol{\xi})\,\phi_{,k}(\mathbf{x})\,d\Omega + \phi_{,k}(\mathbf{x}) = 0 \tag{31}$$

In addition, we may observe that the first two terms in Eq. (22) have the following property:

$$\begin{aligned}&\int_{\partial\Omega} n_i(\boldsymbol{\xi})\,\phi_{,i}(\mathbf{x})\,\phi^*_{,k}(\mathbf{x},\boldsymbol{\xi})\,dS-\int_{\partial\Omega} n_k(\boldsymbol{\xi})\,\phi_{,i}(\mathbf{x})\,\phi^*_{,i}(\mathbf{x},\boldsymbol{\xi})\,dS\\&=\int_{\Omega}\phi_{,i}(\mathbf{x})\,\phi^*_{,ki}(\mathbf{x},\boldsymbol{\xi})\,d\Omega-\int_{\partial\Omega}\phi_{,i}(\mathbf{x})\,\phi^*_{,ik}(\mathbf{x},\boldsymbol{\xi})\,dS\\&=0\end{aligned}\tag{32}$$

By adding Eq. (32) and (31), we have:

$$\begin{aligned}&\int_{\partial\Omega} n_i(\boldsymbol{\xi})\,\phi_{,i}(\mathbf{x})\,\phi^*_{,k}(\mathbf{x},\boldsymbol{\xi})\,dS\\&-\int_{\partial\Omega} n_k(\boldsymbol{\xi})\,\phi_{,i}(\mathbf{x})\,\phi^*_{,i}(\mathbf{x},\boldsymbol{\xi})\,dS\\&+\int_{\partial\Omega}\Theta^*(\mathbf{x},\boldsymbol{\xi})\,\phi_{,k}(\mathbf{x})\,dS\\&+\int_{\Omega} k^2\phi^*(\mathbf{x},\boldsymbol{\xi})\,\phi_{,k}(\mathbf{x})\,d\Omega+\phi_{,k}(\mathbf{x})=0\end{aligned}\tag{33a}$$

or

$$\begin{aligned}&\int_{\partial\Omega} n_i(\boldsymbol{\xi})\,\phi_{,i}(\mathbf{x})\,\phi^*_{,k}(\mathbf{x},\boldsymbol{\xi})\,dS\\&+\int_{\partial\Omega} e_{ikt}D_t\phi(\mathbf{x})\,\phi^*_{,i}(\mathbf{x},\boldsymbol{\xi})\,dS\\&+\int_{\Omega} k^2\phi^*(\mathbf{x},\boldsymbol{\xi})\,\phi_{,k}(\mathbf{x})\,d\Omega+\phi_{,k}(\mathbf{x})=0\end{aligned}\tag{33b}$$

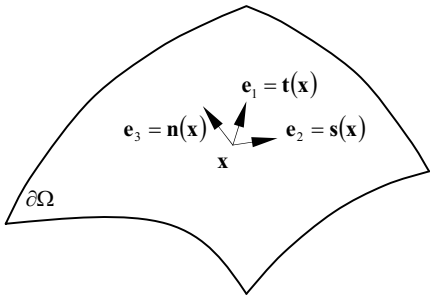

Figure 2 : The local coordinates at a boundary point $\mathbf{x}$

For the numerical implementation purpose, we define the local coordinates at point $\mathbf{x}$ on the boundary $\partial\Omega$, as shown in Fig. 2, and we have $\psi(\mathbf{x})$ in terms of $\phi_{,i}(\mathbf{x})$ on the boundary, as:

$$\begin{cases}\psi_3(\mathbf{x})=q(\mathbf{x})\\ \psi_1(\mathbf{x})=t_i(\mathbf{x})\,\phi_{,i}(\mathbf{x})\\ \psi_2(\mathbf{x})=s_i(\mathbf{x})\,\phi_{,i}(\mathbf{x})\end{cases}\tag{34}$$

in which, the vector $\psi(\mathbf{x})$ in local coordinates comes from two physical terms: the gradient $q(\mathbf{x})$ spans the vector in the outward normal direction, and the gradients of the potential $\phi(\mathbf{x})$ span the vectors in the other two tangential directions.

We rewrite Eq. (33b) as:

$$\begin{aligned}&\int_{\partial\Omega} n_i(\boldsymbol{\xi})\,\psi_i(\mathbf{x})\,\phi^*_{,k}(\mathbf{x},\boldsymbol{\xi})\,dS+\int_{\partial\Omega} e_{ikt}D_t\phi(\mathbf{x})\,\phi^*_{,i}(\mathbf{x},\boldsymbol{\xi})\,dS\\&-\int^{CPV}_{\partial\Omega}\Theta^*(\mathbf{x},\boldsymbol{\xi})\,\phi_{,k}(\mathbf{x})\,dS+\frac{1}{2}\phi_{,k}(\mathbf{x})=0\\&\qquad\qquad\qquad\qquad\mathbf{x}\in\partial\Omega\end{aligned}\tag{35}$$

Using other carefully chosen weak forms of Eq. (12), one can derive any number of "properties" of the fundamental solution [Han and Atluri (2003a)].

We now use the fundamental properties of ϕ^*, as enumerated in this section, to give simple, straightforward and elegant physical and mathematical regularizations of the strongly-singular BIEs for ϕ, and $\phi_{,k}$, as given in Eq. (16) and (22) respectively.

3.4 Regularization of ϕ-BIE, Eq. (16)

In this section, we consider the regularization of ϕ-BIE, as well as the possibility of *satisfying the ϕ-BIE itself in a weak form*, at $\partial\Omega$, through a general Petrov-Galerkin scheme. It is well known the Eq. (16) is numerically tractable if it is restricted only for boundary points, ie., $\mathbf{x}\in\partial\Omega$, because $n_k(\boldsymbol{\xi})\,\phi^*_{,k}(\mathbf{x},\boldsymbol{\xi})$ contains the weak singularity [O $\left(r^{-1}\right)$]. Most researchers have implemented the ϕ-BIE based on this equation and solved the boundary problems. On another hand, considering a domain point which is approaching the boundary, one may encounter the higher singularity [O $\left(r^{-2}\right)$] with Eq. (16).

Subtracting Eq. (26c) from Eq. (16), and obtain:

$$\begin{aligned}&\int_{\partial\Omega} q(\boldsymbol{\xi})\,\phi^*(\mathbf{x},\boldsymbol{\xi})\,dS-\int_{\partial\Omega}\left[\phi(\boldsymbol{\xi})-\phi(\mathbf{x})\right]\Theta^*(\mathbf{x},\boldsymbol{\xi})\,dS\\&+\int_{\Omega} k^2\phi^*(\mathbf{x},\boldsymbol{\xi})\,\phi(\mathbf{x})\,d\Omega=0\end{aligned}\tag{36}$$

With Eq. (28b), Eq. (36) is applicable at point $\mathbf{x}$ on the boundary $\partial\Omega$, as:

$$\int_{\partial\Omega} q(\boldsymbol{\xi})\,\phi^*(\mathbf{x},\boldsymbol{\xi})\,dS - \int_{\partial\Omega} [\phi(\boldsymbol{\xi}) - \phi(\mathbf{x})]\,\Theta^*(\mathbf{x},\boldsymbol{\xi})\,dS = \int_{\partial\Omega}^{CPV} \Theta^*(\mathbf{x},\boldsymbol{\xi})\,\phi(\mathbf{x})\,dS + \frac{1}{2}\phi(\mathbf{x}) \qquad \mathbf{x}\in\partial\Omega \tag{37}$$

One can see that $\phi(\boldsymbol{\xi}) - \phi(\mathbf{x})$ becomes $\mathrm{O}(r)$ when $\boldsymbol{\xi}\to\mathbf{x}$, and thus Eq. 37 becomes weakly-singular [$\mathrm{O}\left(r^{-1}\right)$]. For a point close to the boundary, a reference node on the boundary may be used for regularization [Han and Atluri (2003a)]. Hence, all the integrals in Eq. (37) can be evaluated numerically, for both the boundary points and the points close to the boundary. *We refer to Eq. (37) as the regularized ϕ-BIE or "R-ϕ-BIE".*

On the other hand, when $\partial\Omega$ has corners, ϕ may be expected to have a variation of $r^{+\lambda}(\lambda<1)$ near the corners. In such cases, $\phi(\boldsymbol{\xi}) - \phi(\mathbf{x})$ may become $O\left(r^{\lambda-1}\right)$ when $\boldsymbol{\xi}\to\mathbf{x}$, and thus, in a theoretical sense, Eq. (37) is no longer weakly singular. However, in a numerical solution of R-ϕ-BIE (37) directly, through a collocation process, to derive a ϕ Boundary Element Method (BEM-R-ϕ-BIE), we envision using only C^0 polynomial interpolations of ϕ and q. Thus, in the numerical implementation of the *BEM-R-ϕ-BIE by a collocation of Eq. (37)*, we encounter only weakly singular integrals. This method of BEM-R-ϕ-BIE, using a direct collocation of (37), is presented elsewhere [Qian, Han, and Atluri (2003)]. By using C^0 elements and employing an adaptive boundary-element refinement strategy near corners at the boundary, one may extract the value of $(\lambda<1)$ in the asymptotic solution for ϕ near such a corner.

We can also use a Petrov-Galerkin scheme to write the weak-form for Eq. (37) as:

$$\int_{\partial\Omega} w(\mathbf{x})\,dS_x \int_{\partial\Omega} q(\boldsymbol{\xi})\,\phi^*(\mathbf{x},\boldsymbol{\xi})\,dS_\xi - \int_{\partial\Omega} w(\mathbf{x})\,dS_x \int_{\partial\Omega} [\phi(\boldsymbol{\xi}) - \phi(\mathbf{x})]\,\Theta^*(\mathbf{x},\boldsymbol{\xi})\,dS_\xi = \int_{\partial\Omega} w(\mathbf{x})\,dS_x \int_{\partial\Omega}^{CPV} \Theta^*(\mathbf{x},\boldsymbol{\xi})\,\phi(\mathbf{x})\,dS_\xi + \frac{1}{2}\int_{\partial\Omega} w(\mathbf{x})\,\phi(\mathbf{x})\,dS_x \tag{38}$$

where $w(\mathbf{x})$ is a test function on the boundary $\partial\Omega$. If$w(\mathbf{x})$is chosen as a Dirac delta function, i.e., $w(\mathbf{x}) = \delta(\mathbf{x},\mathbf{x}_m)$ at$\partial\Omega$, we obtain the standard "collocation" boundary element method, i.e., BEM-R-ϕ-BIE mentioned earlier. The collocation BEM-R-ϕ-BIE method and the attendant numerical details are presented elsewhere [Qian, Han, and Atluri (2003)]. In the present paper, we consider the general Petrov-Galerkin weak solutions of the weakly singular ϕ-BIE.

By using Eq. (28b), we may obtain from Eq. (38):

$$\frac{1}{2}\int_{\partial\Omega} w(\mathbf{x})\,\phi(\mathbf{x})\,dS_x = \int_{\partial\Omega} w(\mathbf{x})\,dS_x \int_{\partial\Omega} q(\boldsymbol{\xi})\,\phi^*(\mathbf{x},\boldsymbol{\xi})\,dS_\xi - \int_{\partial\Omega} w(\mathbf{x})\,dS_x \int_{\partial\Omega}^{CPV} \Theta^*(\mathbf{x},\boldsymbol{\xi})\,\phi(\boldsymbol{\xi})\,dS_\xi \tag{39}$$

If $w(\mathbf{x})$ is chosen to be identical to a function which is energy-conjugate to $\phi(\mathbf{x})$, viz. the trial function , we obtain the symmetric Galerkin ϕ-BIE form as [Han and Atluri 2003a)]

$$\frac{1}{2}\int_{\partial\Omega} \hat{q}(\mathbf{x})\,\phi(\mathbf{x})\,dS_x = \int_{\partial\Omega} \hat{q}(\mathbf{x})\,dS_x \int_{\partial\Omega} q(\boldsymbol{\xi})\,\phi^*(\mathbf{x},\boldsymbol{\xi})\,dS_\xi - \int_{\partial\Omega} \hat{q}(\mathbf{x})\,dS_x \int_{\partial\Omega}^{CPV} \Theta^*(\mathbf{x},\boldsymbol{\xi})\,\phi(\boldsymbol{\xi})\,dS_\xi \tag{40}$$

Eq. (40) leads to the present novel formulation for a Symmetric Galerkin Boundary Element Method for the weakly singular BEM-R-ϕ-BIE. *We label this as SGBEM-R-ϕ-BIE for convenience.*

3.5 Regularization of q-BIE, Eq. (21)

By subtracting Eq. (24) from Eq. (35), we can obtain the fully regularized form of Eq. (24) as:

$$\int_{\partial\Omega}\left[q\left(\boldsymbol{\xi}\right)-n_i\left(\boldsymbol{\xi}\right)\psi_i\left(\mathbf{x}\right)\right]\phi^*_{,k}\left(\mathbf{x},\boldsymbol{\xi}\right)dS$$
$$+\int_{\partial\Omega}e_{ikt}\left[D_t\phi\left(\boldsymbol{\xi}\right)-\left(D_t\phi\right)\left(\mathbf{x}\right)\right]\phi^*_{,i}\left(\mathbf{x},\boldsymbol{\xi}\right)dS$$
$$+\int_{\partial\Omega}k^2n_k\left(\boldsymbol{\xi}\right)\phi\left(\boldsymbol{\xi}\right)\phi^*\left(\mathbf{x},\boldsymbol{\xi}\right)dS$$
$$+\int_{\partial\Omega}^{CPV}\Theta^*\left(\mathbf{x},\boldsymbol{\xi}\right)q\left(\mathbf{x}\right)dS+\frac{1}{2}q\left(\mathbf{x}\right)=0 \tag{41}$$

We define a kernel function as:

$$\hat{\Theta}^*\left(\mathbf{x},\boldsymbol{\xi}\right)=-\frac{\partial\phi^*\left(\mathbf{x},\boldsymbol{\xi}\right)}{\partial n_x}=n_k\left(\mathbf{x}\right)\frac{\partial\phi^*\left(\mathbf{x},\boldsymbol{\xi}\right)}{\partial\xi_k} \tag{42}$$

If we contract with $n_k\left(\mathbf{x}\right)$ on both sides of Eq. (41), we obtain

$$\int_{\partial\Omega}\left[q\left(\boldsymbol{\xi}\right)-n_i\left(\boldsymbol{\xi}\right)\psi_i\left(\mathbf{x}\right)\right]\hat{\Theta}^*\left(\mathbf{x},\boldsymbol{\xi}\right)dS$$
$$+\int_{\partial\Omega}\left[D_t\phi\left(\boldsymbol{\xi}\right)-\left(D_t\phi\right)\left(\mathbf{x}\right)\right]n_k\left(\mathbf{x}\right)e_{ikt}\phi^*_{,i}\left(\mathbf{x},\boldsymbol{\xi}\right)dS$$
$$+\int_{\partial\Omega}k^2n_k\left(\mathbf{x}\right)n_k\left(\boldsymbol{\xi}\right)\phi\left(\boldsymbol{\xi}\right)\phi^*\left(\mathbf{x},\boldsymbol{\xi}\right)dS$$
$$+\int_{\partial\Omega}^{CPV}\Theta^*\left(\mathbf{x},\boldsymbol{\xi}\right)q\left(\mathbf{x}\right)dS+\frac{1}{2}q\left(\mathbf{x}\right)=0 \tag{43}$$

We label Eq. (43) as the regularized q-BIE, or "R-q-BIE". When $\partial\Omega$ is smooth, one can see that $\left[q\left(\boldsymbol{\xi}\right)-n_i\left(\boldsymbol{\xi}\right)\psi_i\left(\mathbf{x}\right)\right]$ and $\left[D_t\phi\left(\boldsymbol{\xi}\right)-\left(D_t\phi\right)\left(\mathbf{x}\right)\right]$ become $O\left(r\right)$ when $\boldsymbol{\xi}\rightarrow\mathbf{x}$, and Eq. 41 becomes weakly singular $\left[O\left(r^{-1}\right)\right]$ on a 3D problem. Thus, all the integrals in Eq. 43 can be evaluated numerically, and applicable to any point $\mathbf{x}$ on the boundary $\partial\Omega$. On the other hand, when $\partial\Omega$ has corners, $\left[q\left(\boldsymbol{\xi}\right)-n_i\left(\boldsymbol{\xi}\right)\psi_i\left(\mathbf{x}\right)\right]$ and $\left[D_t\phi\left(\boldsymbol{\xi}\right)-\left(D_t\phi\right)\left(\mathbf{x}\right)\right]$ may become $O\left(r^{\lambda-1}\right)$ when $\boldsymbol{\xi}\rightarrow\mathbf{x}$, and thus, in a theoretical sense, Eq. 43 is no longer weakly singular. However, in a numerical implementation of the R-q-BIE, viz. Eq. (43), directly, *through a collocation process, to derive a qBoundary Element Method (BEM-R-q-BIE)*, we envision using only C^0 polynomial interpolations of ϕ and q. Thus, in the numerical implementation of the BEM-q-BIE by a collocation of Eq. (43), we encounter only weakly singular integrals. The method of BEM-R-q-BIE using a direct collocation of Eq. (43), is presented elsewhere [Qian, Han, and Atluri (2003)].

We can also use a Petrov-Galerkin scheme to write a weak form for Eq. (43) as:

$$\int_{\partial\Omega}w\left(\mathbf{x}\right)dS_x\int_{\partial\Omega}\left[D_t\phi\left(\boldsymbol{\xi}\right)-\left(D_t\phi\right)\left(\mathbf{x}\right)\right]n_k\left(\mathbf{x}\right)e_{ikt}\phi^*_{,i}\left(\mathbf{x},\boldsymbol{\xi}\right)dS_\xi$$
$$+\int_{\partial\Omega}w\left(\mathbf{x}\right)dS_x\int_{\partial\Omega}\left[q\left(\boldsymbol{\xi}\right)-n_i\left(\boldsymbol{\xi}\right)\psi_i\left(\mathbf{x}\right)\right]\hat{\Theta}^*\left(\mathbf{x},\boldsymbol{\xi}\right)dS_\xi$$
$$+\int_{\partial\Omega}w\left(\mathbf{x}\right)dS_x\int_{\partial\Omega}k^2n_k\left(\mathbf{x}\right)n_k\left(\boldsymbol{\xi}\right)\phi\left(\boldsymbol{\xi}\right)\phi^*\left(\mathbf{x},\boldsymbol{\xi}\right)dS_\xi$$
$$+\int_{\partial\Omega}w\left(\mathbf{x}\right)dS_x\int_{\partial\Omega}^{CPV}\Theta^*\left(\mathbf{x},\boldsymbol{\xi}\right)q\left(\mathbf{x}\right)dS_\xi$$
$$+\frac{1}{2}\int_{\partial\Omega}w\left(\mathbf{x}\right)q\left(\mathbf{x}\right)dS_x=0 \tag{44}$$

where $w\left(\mathbf{x}\right)$ is a test function. If $w\left(\mathbf{x}\right)$ is chosen as a Dirac delta function, i.e., $w\left(\mathbf{x}\right)=\delta\left(\mathbf{x},\mathbf{x}_m\right)$ at$\partial\Omega$, we obtain the standard "collocation" boundary element method. [BEM-R-q-BIE]

Also, we can directly use a Petrov-Galerkin scheme to write a weak-form for Eq. (24) as:

$$-\int_{\partial\Omega}q\left(\mathbf{x}\right)w\left(\mathbf{x}\right)dS_x=\int_{\partial\Omega}w\left(\mathbf{x}\right)dS_x\int_{\partial\Omega}q\left(\boldsymbol{\xi}\right)\hat{\Theta}^*\left(\mathbf{x},\boldsymbol{\xi}\right)dS_\xi$$
$$+\int_{\partial\Omega}w\left(\mathbf{x}\right)dS_x\int_{\partial\Omega}D_t\phi\left(\boldsymbol{\xi}\right)e_{ikt}n_k\left(\mathbf{x}\right)\phi^*_{,i}\left(\mathbf{x},\boldsymbol{\xi}\right)dS_\xi$$
$$+\int_{\partial\Omega}w\left(\mathbf{x}\right)dS_x\int_{\partial\Omega}k^2n_k\left(\boldsymbol{\xi}\right)\phi\left(\boldsymbol{\xi}\right)n_k\left(\mathbf{x}\right)\phi^*\left(\mathbf{x},\boldsymbol{\xi}\right)dS_\xi \tag{45}$$

The first integral at the right side of Eq. (45) can be written as:

$$\int_{\partial\Omega}w\left(\mathbf{x}\right)dS_x\int_{\partial\Omega}q\left(\boldsymbol{\xi}\right)\hat{\Theta}^*\left(\mathbf{x},\boldsymbol{\xi}\right)dS_\xi$$
$$=\int_{\partial\Omega}q\left(\boldsymbol{\xi}\right)dS_\xi\int_{\partial\Omega}^{CPV}w\left(\mathbf{x}\right)\hat{\Theta}^*\left(\mathbf{x},\boldsymbol{\xi}\right)dS_x$$
$$-\int_{\partial\Omega}\frac{1}{2}q\left(\mathbf{x}\right)w\left(\mathbf{x}\right)dS_x \tag{46}$$

in which Eq. (28b) is used, and $\frac{\partial}{\partial x_i}=-\frac{\partial}{\partial\xi_i}$.

The second integral on the right side of Eq. (45), can be simplified by using the Stokes theorem. We introduce a kernel function, Σ^*_{kt}, defined as

$$\begin{aligned}\Sigma^*_{kt}(\mathbf{x},\boldsymbol{\xi}) &= e_{ikt}\phi^*_{,i}(\mathbf{x},\boldsymbol{\xi}) \\ &= e_{ink}\left(-\delta_{nt}\phi^*_{,i}(\mathbf{x},\boldsymbol{\xi})\right) \\ &= e_{ink}\mathrm{H}^*_{nt,i}(\mathbf{x},\boldsymbol{\xi}) \end{aligned} \tag{47}$$

Thus, by definition, $\mathrm{H}^*_{nt}(\mathbf{x},\boldsymbol{\xi}) = -\delta_{nt}\phi^*(\mathbf{x},\boldsymbol{\xi})$, and this kernel function is seen to be:

$$\mathrm{H}^*_{nt}(\mathbf{x},\boldsymbol{\xi}) = -\frac{i}{4}H^{(1)}_0(kr)\,\delta_{nt} \quad \text{in 2D} \tag{48a}$$

and

$$\mathrm{H}^*_{nt}(\mathbf{x},\boldsymbol{\xi}) = -\frac{e^{-ikr}}{4\pi r}\delta_{nt} \quad \text{in 3D} \tag{48b}$$

The second integral on the right side of Eq. (45) is rewritten as

$$\begin{aligned}&\int_\Omega w(\mathbf{x})\,dS_x \int_\Omega D_t\phi(\boldsymbol{\xi})\,e_{ikt}n_k(\mathbf{x})\,\phi^*_{,i}(\mathbf{x},\boldsymbol{\xi})\,dS_\xi \\ &= \int_\Omega D_k w(\mathbf{x})\,dS_x \int_\Omega D_t\phi(\boldsymbol{\xi})\,\mathrm{H}_{kt}(\mathbf{x},\boldsymbol{\xi})\,dS_\xi \end{aligned} \tag{49}$$

Then, through combining Eq. (45), (46) and (49), the final equation becomes:

$$\begin{aligned}&-\frac{1}{2}\int_\Omega q(\mathbf{x})\,w(\mathbf{x})\,dS_x \\ &= \int_\Omega q(\boldsymbol{\xi})\,dS_\xi \int_\Omega^{CPV} w(\mathbf{x})\,\hat{\Theta}^*(\mathbf{x},\boldsymbol{\xi})\,dS_x \\ &+ \int_\Omega D_k w(\mathbf{x})\,dS_x \int_\Omega D_t\phi(\boldsymbol{\xi})\,\mathrm{H}_{kt}(\mathbf{x},\boldsymbol{\xi})\,dS_\xi \\ &+ \int_\Omega w(\mathbf{x})\,dS_x \int_\Omega k^2 n_k(\boldsymbol{\xi})\,\phi(\boldsymbol{\xi})\,n_k(\mathbf{x})\,\phi^*(\mathbf{x},\boldsymbol{\xi})\,dS_\xi \end{aligned} \tag{50}$$

If the test function $w(\mathbf{x})$ is chosen to be identical to a function which is energy-conjugate to $q(\mathbf{x})$, viz. the trial function $\hat{\phi}(\mathbf{x})$, we obtain the symmetric Galerkin q-BIE form as

$$\begin{aligned}&-\frac{1}{2}\int_\Omega q(\mathbf{x})\,\hat{\phi}(\mathbf{x})\,dS_x \\ &= \int_\Omega q(\boldsymbol{\xi})\,dS_\xi \int_\Omega^{CPV} \hat{\phi}(\mathbf{x})\,\hat{\Theta}^*(\mathbf{x},\boldsymbol{\xi})\,dS_x \\ &+ \int_\Omega D_k\hat{\phi}(\mathbf{x})\,dS_x \int_\Omega D_t\phi(\boldsymbol{\xi})\,\mathrm{H}_{kt}(\mathbf{x},\boldsymbol{\xi})\,dS_\xi \\ &+ \int_\Omega n_k(\mathbf{x})\,\hat{\phi}(\mathbf{x})\,dS_x \int_\Omega k^2 n_k(\boldsymbol{\xi})\,\phi(\boldsymbol{\xi})\,\phi^*(\mathbf{x},\boldsymbol{\xi})\,dS_\xi \end{aligned} \tag{51}$$

Eq. (51) leads to the present novel formulation for a Symmetric Galerkin Boundary Element Method for the regularized R-q-BIE. *We label this as "SGBEM-R-q-BIE" for convenience, in this paper.*

3.6 Some detailed properties of kernel functions

3.6.1 $\Theta^*(\mathbf{x},\boldsymbol{\xi})$ *and* $\hat{\Theta}^*(\mathbf{x},\boldsymbol{\xi})$

First of all, it is quite straight forward to see that

$$\Theta^*(\mathbf{x},\boldsymbol{\xi}) = -\hat{\Theta}^*(\boldsymbol{\xi},\mathbf{x}) \tag{52}$$

from the definition of $\Theta^*(\mathbf{x},\boldsymbol{\xi})$ and $\hat{\Theta}^*(\mathbf{x},\boldsymbol{\xi})$. Eq. (52) results in the symmetry of the "SGBEM-R-ϕ-BIE" and "SGBEM-R-q-BIE", as seen in the next section.

3.6.2 $\mathrm{H}^*(\mathbf{x},\boldsymbol{\xi})$

¿From the definition of $\Sigma^*(\mathbf{x},\boldsymbol{\xi})$ in Eq. (47), we know that

$$\nabla\cdot\Sigma^*(\mathbf{x},\boldsymbol{\xi}) = 0 \tag{53a}$$

$$\Sigma^*(\mathbf{x},\boldsymbol{\xi}) = \nabla\times\mathrm{H}^*(\mathbf{x},\boldsymbol{\xi}) \tag{53b}$$

which means that $\Sigma^*(\mathbf{x},\boldsymbol{\xi})$ spans a solenoidal field, and there exists a potential field, in this case, $\mathrm{H}^*(\mathbf{x},\boldsymbol{\xi})$, to construct the solenoidal field by using a curl operator. These properties ensure the application of the Stokes theorem in Eq. (49) to obtain simplified boundary integral equations.

Also, $\mathrm{H}^*(\mathbf{x},\boldsymbol{\xi})$ becomes $O\left(r^{-1}\right)$ in 3 dimensional problem, which is of the same order as $\phi^*(\mathbf{x},\boldsymbol{\xi})$, when $\boldsymbol{\xi}\to\mathbf{x}$. Therefore, $\mathrm{H}^*(\mathbf{x},\boldsymbol{\xi})$ possesses the weak singularity, and it is convenient for the numerical implementation.

Now, the ϕ-BIE and the q-BIE have been fully desingularized simply, and elegantly in the present work.

3.7 Numerical Details of the "SGBEM-R-ϕ-BIE" and "SGBEM-R-q-BIE"

Let the regular boundary S be partitioned into a portion S_p on which potential is prescribed, and a portion S_q where velocity potential gradients are prescribed. We apply the ϕ-BIE weak form on S_p with $\hat{q}=0$ on S_q, and the q-BIE weak form on S_q with $\hat{\phi}=0$ on S_p. Thus we obtain:

$$\begin{aligned}
&\int_{S_p}\hat{q}(\mathbf{x})\int_{S_p}q(\boldsymbol{\xi})\,\phi^*(\mathbf{x},\boldsymbol{\xi})\,dS_\xi dS_x\\
&-\int_{S_p}\hat{q}(\mathbf{x})\int_{S_q}^{CPV}\Theta^*(\mathbf{x},\boldsymbol{\xi})\,\phi(\boldsymbol{\xi})\,dS_\xi dS_x\\
&=\frac{1}{2}\int_{S_p}\hat{q}(\mathbf{x})\,\phi(\mathbf{x})\,dS_x-\int_{S_p}\hat{q}(\mathbf{x})\int_{S_q}q(\boldsymbol{\xi})\,\phi^*(\mathbf{x},\boldsymbol{\xi})\,dS_\xi dS_x\\
&+\int_{S_p}\hat{q}(\mathbf{x})\int_{S_p}^{CPV}\Theta^*(\mathbf{x},\boldsymbol{\xi})\,\phi(\boldsymbol{\xi})\,dS_\xi dS_x
\end{aligned}\tag{54a}$$

$$\begin{aligned}
&\int_{S_q}q(\boldsymbol{\xi})\int_{S_p}^{CPV}\hat{\phi}(\mathbf{x})\,\hat{\Theta}^*(\mathbf{x},\boldsymbol{\xi})\,dS_x dS_\xi\\
&+\int_{S_q}D_k\hat{\phi}(\mathbf{x})\int_{S_q}D_t\phi(\boldsymbol{\xi})\,\mathrm{H}_{kt}(\mathbf{x},\boldsymbol{\xi})\,dS_\xi dS_x\\
&+\int_{S_q}n_k(\mathbf{x})\,\hat{\phi}(\mathbf{x})\int_{S_q}k^2n_k(\boldsymbol{\xi})\,\phi(\boldsymbol{\xi})\,\phi^*(\mathbf{x},\boldsymbol{\xi})\,dS_\xi dS_x\\
&=-\frac{1}{2}\int_{S_q}q(x)\,\hat{\phi}(\mathbf{x})\,dS_x\\
&-\int_{S_q}q(\boldsymbol{\xi})\int_{S_q}^{CPV}\hat{\phi}(\mathbf{x})\,\hat{\Theta}^*(\mathbf{x},\boldsymbol{\xi})\,dS_x dS_\xi\\
&-\int_{S_q}D_k\hat{\phi}(\mathbf{x})\int_{S_p}D_t\phi(\boldsymbol{\xi})\,\mathrm{H}_{kt}(\mathbf{x},\boldsymbol{\xi})\,dS_\xi dS_x\\
&-\int_{S_q}n_k(\mathbf{x})\,\hat{\phi}(\mathbf{x})\int_{S_p}k^2n_k(\boldsymbol{\xi})\,\phi(\boldsymbol{\xi})\,\phi^*(\mathbf{x},\boldsymbol{\xi})\,dS_\xi dS_x
\end{aligned}\tag{54b}$$

Due to the properties of the kernel functions, with the symmetric features of the Eq. (54a) and (54b), *the symmetry of the "SGBEM-R-ϕ-BIE" and "SGBEM-R-q-BIE" equations is guaranteed.*

4 Numerical results

In the implementation of the "SGBEM-R-ϕ-BIE" and "SGBEM-R-q-BIE", another key step is to evaluate the double area integrals of the weakly singular kernels. An efficient approach for triangular boundary elements, which is based on coordinate transformations, is presented by [Andra (1998); Erichsen and Sauter (1998)]. The transformation Jacobian cancels the weak singularity of the kernels. The method used in this paper is based on the approach presented in [Nikishkov, Park, and Atluri (2001)], which is designed for *quadrilateral boundary elements*. For coincident elements and for elements with common edges or common vertices, the four-dimensional integration domain is divided into several integration subdomains. In each subdomain, a special coordinate transformation is introduced, which cancels the singularity.

In order to check the accuracy and efficiency of the proposed method, three different acoustic problems are considered: (1) acoustic field radiated by a sphere with driving and admittance surfaces; (2) the standard pulsating sphere problem; and (3) acoustic scattering from the surface of a solid cone and a cube.

4.1 Application to radiation

4.1.1 Acoustic field radiated by a sphere with driving and admittance surfaces

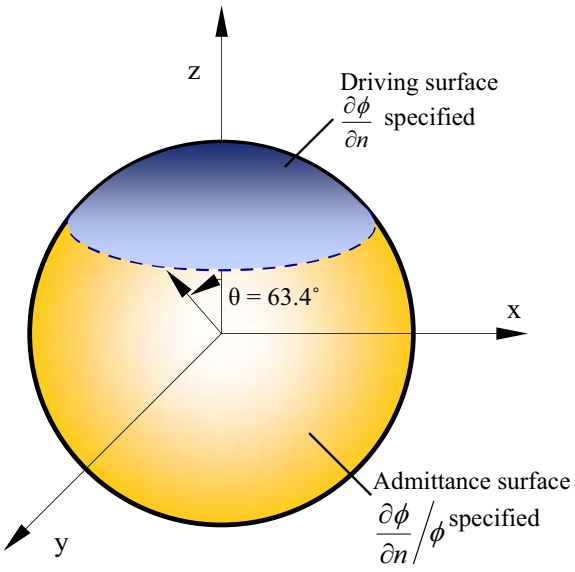

Figure 3 : Specifications of boundary conditions on the surface of the sphere

The sound field radiated by a sphere is studied in this section. The sphere is of unit radius with both a driving

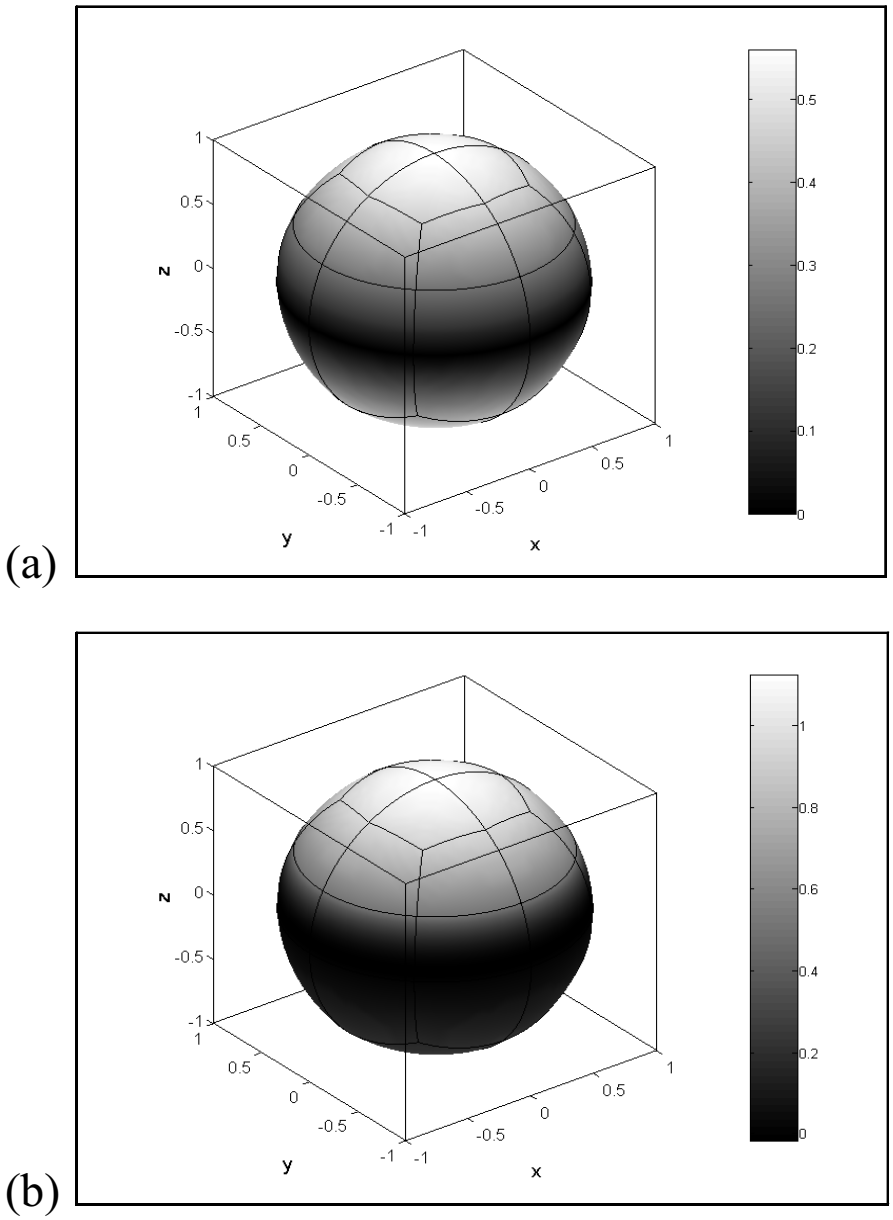

Figure 4 : Numerical solution by SGBEM-R-ϕ-BIE & SGBEM-R-q-BIE of (a) $|\phi|$; (b) $\left|\frac{\partial\phi}{\partial n}\right|$ on the surface

surface as well as an admittance surface (Fig. 3), which constitute discontinuous boundary conditions. This numerical example is commonly used, because the exact solution is known [Meyer, Bell, Zinn, and Stallybrass (1978)]

To check the numerical approach and the computer code, the first case of the radiated field, with the wave number $k = 2$ is investigated. 32 8-node quadrilateral elements are employed in the present boundary element model. The exact solution for the conditions:

Driving surface:

$$\frac{\partial\phi}{\partial n} = (0.0385 + 1.12i)\cos\theta$$

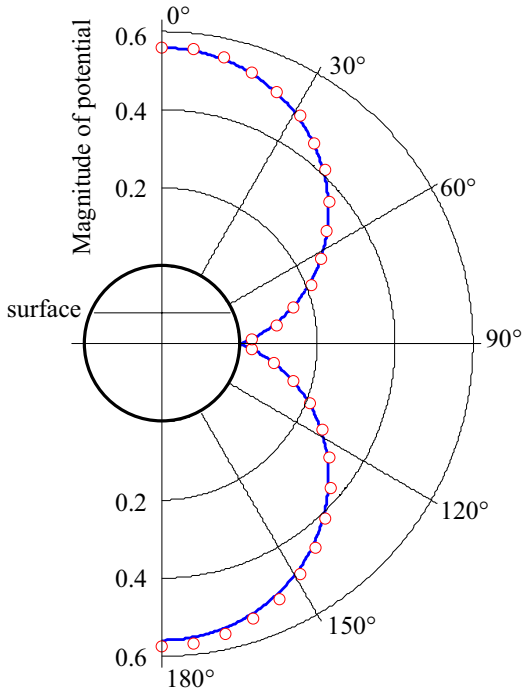

Figure 5 : Exact and numerical solution of $|\phi|$ for k = 2: -, Exact; o, SGBEM-R-ϕ-BIE & SGBEM-R-q-BIE

Admittance surface:

$$\frac{\partial \phi}{\partial n} = (-1.2 + 1.6i)\,\phi$$

is given by:

$\phi = (0.435 - 0.351i)\cos\theta$ on the surface, and

$\phi = (-0.00867 + 0.00498i)\cos\theta$ at the far field ($kr = 100$).

The solution of this case is θ dependent, as shown in Fig. 4. A comparison between the numerical and exact solutions for the amplitude $|\phi|$ of the velocity potential on the surface of the sphere is presented in Fig. 5, wherein excellent agreement between the two solutions is noted.

The second case of a radiating sphere is studied at the wave number $k = 4.49$ (the second internal eigenvalue of the sphere, and the first eigenvalue is π), which has the largest value of error ($\sim 14\%$) in the numerical solution of [Meyer, Bell, Zinn, and Stallybrass (1978)]. The exact solution for the radiated field, for the given conditions:

Driving surface:

$$\frac{\partial \phi}{\partial n} = (-0.976 - 0.239i)\cos\theta$$

Admittance surface:

$$\frac{\partial \phi}{\partial n} = (-1.05 + 4.28i)\,\phi$$

is given by:

$\phi = 0.228i\cos\theta$ on the surface, and

$\phi = (-0.00867 + 0.00498i)\cos\theta$ at the far field ($kr = 100$).

A comparison between the conventional collocation-based boundary integral equations (ϕ-BIE) viz., the BEM-R-ϕ-BIE approach, the present SGBEM-R-ϕ-BIE and SGBEM-R-q-BIE, and the exact solutions, for the amplitude $|\phi|$ of the velocity potential on the surface and at the far field of the sphere is presented in Fig. 6. The excellent agreement between the present SGBEM solutions and the exact solution is noted. And, the results also show the very high accuracy at the characteristic frequencies, of the present SGBEM method in comparison to the conventional boundary element method, i.e., the BEM-R-ϕ-BIE method. The agreement of the proposed method with that of the exact solution is superior to that of the numerical solution of Meyer, Bell, Zinn, and Stallybrass (1978).

4.1.2 Application to a pulsating sphere

The field radiated from a pulsating sphere into the infinite homogeneous medium is chosen as an example for the exterior problem. The analytical solution of the acoustic pressure for a sphere of radius a, pulsating with uniform radial velocity v_a, is given by [Chien, Rajiyah, and Atluri (1990)]

$$\frac{p(r)}{z_0 v_a} = \frac{a}{r}\frac{ika}{1+ika}e^{-ik(r-a)} \tag{55}$$

where z_0 is the characteristic impedance, $p(r)$ is the acoustic pressure at distance r, and k is the wave number. In this example, the hatched area on the surface in Fig. 7 is assigned the Dirichlet boundary condition (using SGBEM-R-ϕ-BIE correspondingly), and the remained area on the surface is assigned the Neumann condition (using SGBEM-R-q-BIE correspondingly). The

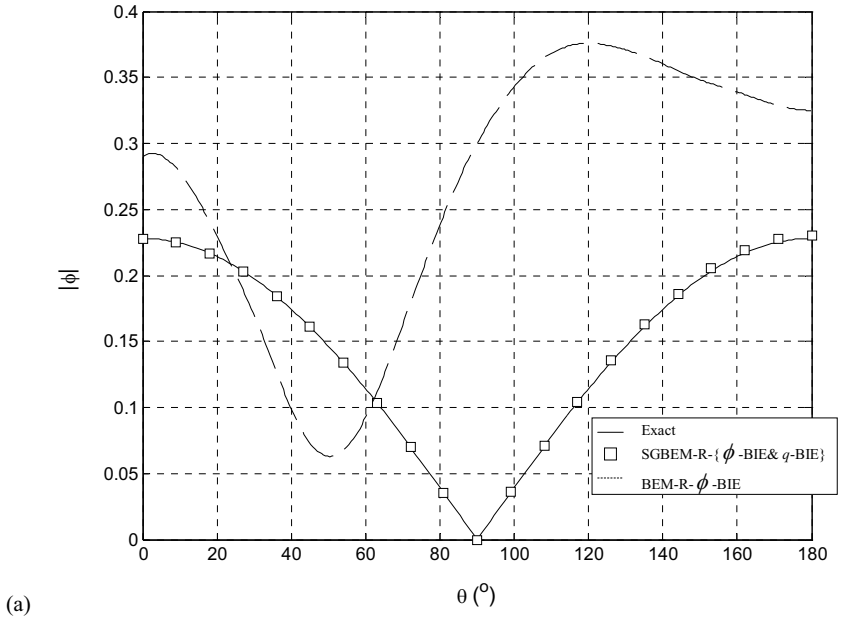

(a)

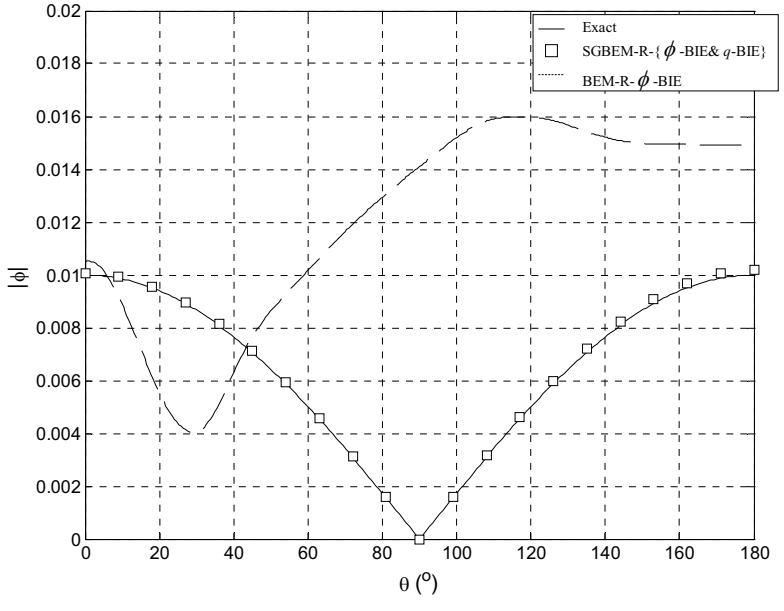

(b)

Figure 6 : Solutions of $|\phi|$: (a) on the surface and (b) at the far field (kr=100); k = 4.49

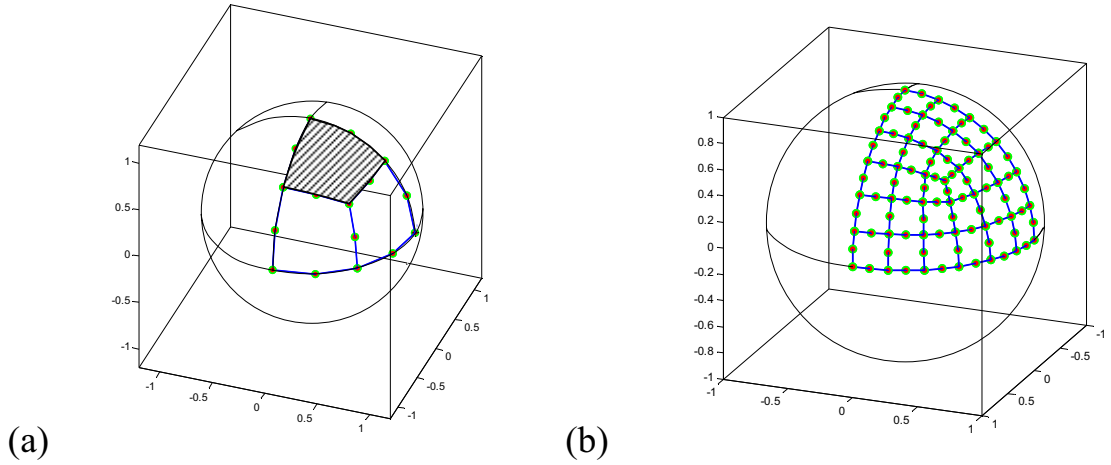

Figure 7 : Surface discretization with quadrilateral elements (a) 24 element model; (b) 216 element model

whole sphere is considered for modeling: a 24 element model and a 216 element model, as shown in Fig. 7. The models are discretized by using 8-node isoparametric quadrilateral elements. The evaluation of all integrals of kernels is performed by using 3x3 Gaussian quadrature.

In Fig. 8 and Fig. 9, the real and imaginary parts of dimensionless surface acoustic pressures are plotted with respect to the reduced frequency *ka*. Fig. 8 presents the numerical solutions with 24 elements, while results with 216 elements are plotted in Fig. 9. The present results are seen to converge to the analytical solution, with a mesh refinement. It is obvious that the conventional BIE method fails to provide unique solutions near $k = \pi, 2\pi \cdots$, which is also demonstrated in many earlier works, such as [Yan, Hung, and Zheng (2003)]. There is a good agreement between the present SGBEM solutions and exact solution with *ka* up to 7.5.

4.2 Application to scattering

4.2.1 Scattering of pressure field around a solid cone

To test the capability of handling the sharp corners by the proposed SGBEM method, the acoustic scattering of plane waves with unit amplitude (e^{-ikx}) along the axis of a truncated ordinary cone with base radius $r_b = 1$ and a much smaller top radius $r_t = 0.1$ as shown in Fig. 10, is studied in this example. To make the method to be applicable to scattering problem, only a small change is necessary to Eq. (40) as:

$$\begin{aligned}
&\frac{1}{2}\int_{\partial\Omega} \hat{q}(\mathbf{x})\,\phi(\mathbf{x})\,dS_x - \int_{\partial\Omega} \hat{q}(\mathbf{x})\,\phi^i(\mathbf{x})\,dS_x \\
&= \int_{\partial\Omega} \hat{q}(\mathbf{x})\,dS_x \int_{\partial\Omega} q(\boldsymbol{\xi})\,\phi^*(\mathbf{x},\boldsymbol{\xi})\,dS_\xi \\
&- \int_{\partial\Omega} \hat{q}(\mathbf{x})\,dS_x \int_{\partial\Omega}^{CPV} \Theta^*(\mathbf{x},\boldsymbol{\xi})\,\phi(\boldsymbol{\xi})\,dS_\xi
\end{aligned} \tag{56}$$

where $\phi^i(\mathbf{x})$ is the incident acoustic potential, and also a similar change to Eq. (51) is needed.

For comparison purposes, 3 different-sized models are used for $ka = 1$ (92 elements; 318 elements; 952 elements). The analytical solution for the above problem is unavailable and hence the solution at the horizontal plane of symmetry, which is aligned with the incoming wave, is studied. The non-dimensionalized scattered pressure p_s/p_i, at distance r from the center of the cone, versus the polar angle is plotted in Fig. 13 for non-dimensionalized wave number $ka = 1.0$. The solution shows that the method converges, as the number of elements increases.

To deal with the non-smooth boundary, i.e., the discontinuity of normal gradient of the pressure in this case, we must note that the degrees of freedom at the discontinuous points should not be mixed or combined. There is no other special treatment required for the discontinuous boundary. This example shows that the SGBEM-R-ϕ-BIE and SGBEM-R-q-BIE methods are applicable to scattering problems. One of the advantages of the present method is that no discontinuous element is re-

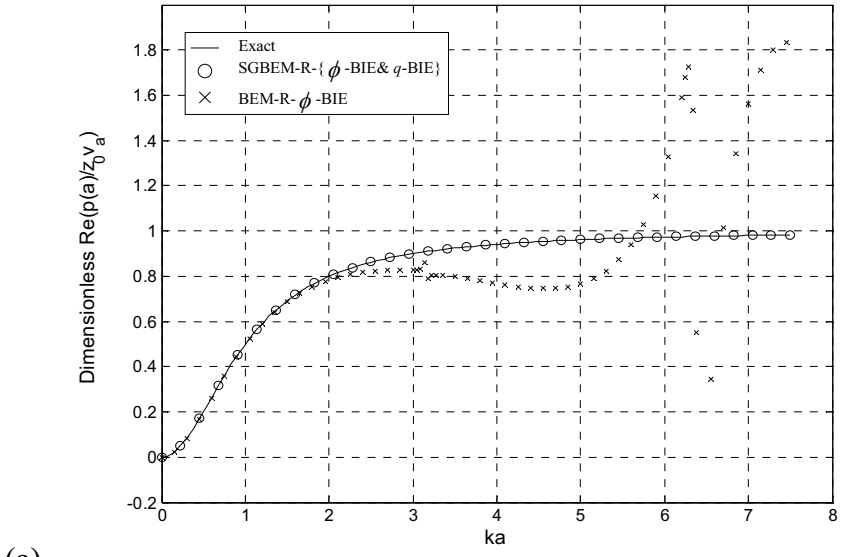

(a)

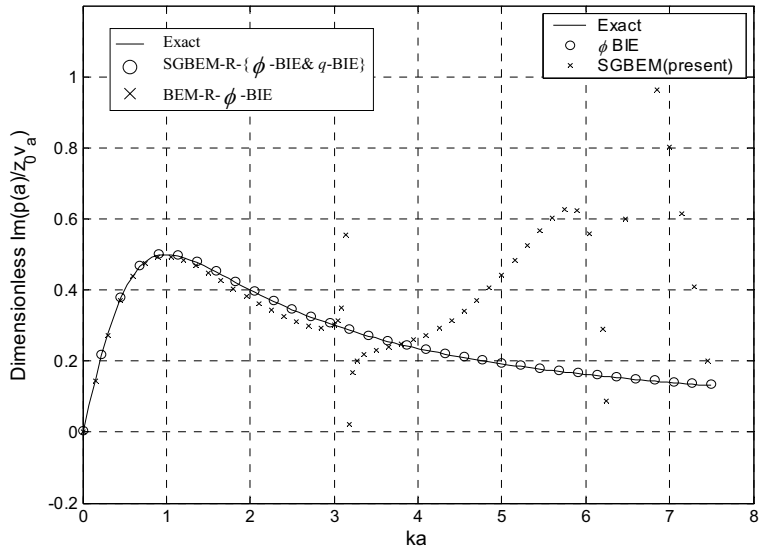

(b)

Figure 8 : Dimensionless surface acoustic pressure of a pulsating (24 elements): (a) real part; (b) imaginary part

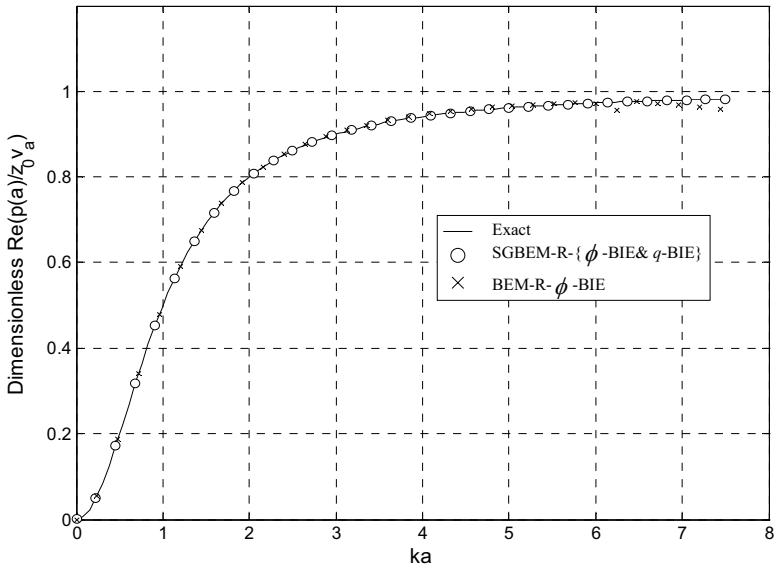

(a)

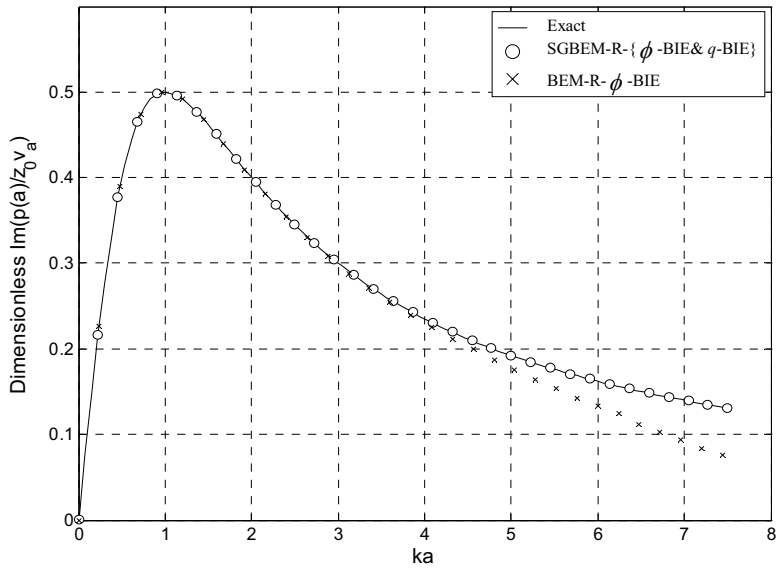

(b)

Figure 9 : Dimensionless surface acoustic pressure of a pulsating sphere (216 elements): (a) real part; (b) imaginary part

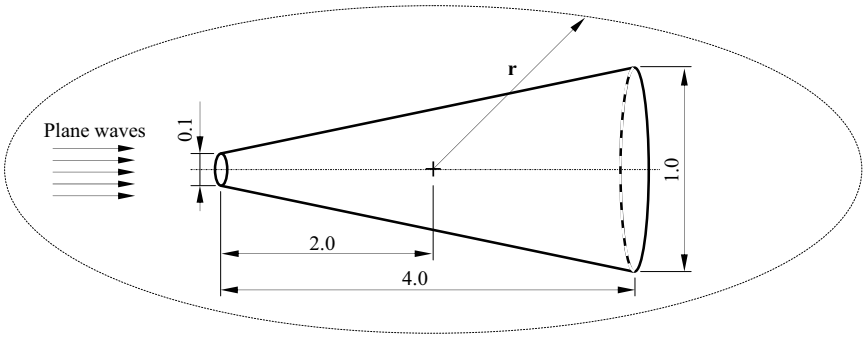

Figure 10 : The geometry of the truncated ordinary cone

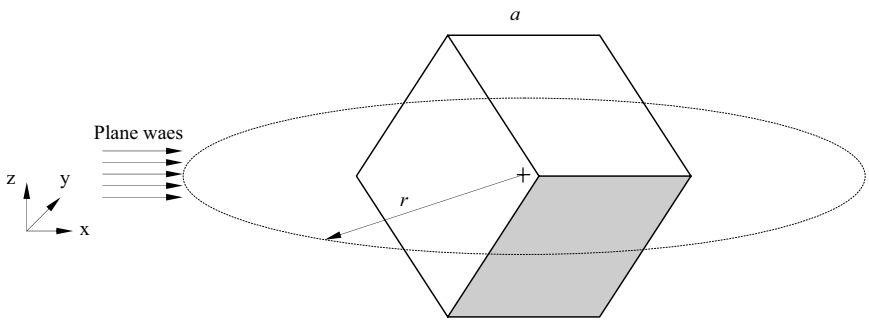

Figure 11 : The geometry and the location of the cube

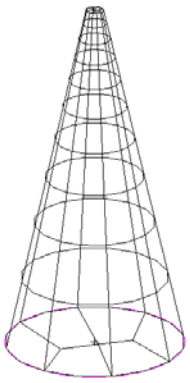

Figure 12 : The surface discretization of the cone with 92 8-node quadrilateral elements

quired for solving the non-smooth boundary problem. Further more, in the widely used collocation method, the coefficients $(1/2)$ in Eq. (39) and (50) actually work for smooth boundary only, and they shall be assigned different values for the respective geometries [for instance, $\theta/4\pi$ for a sharp corner with subtended solid angle θ]. However, this coefficient change won't arise in the present SGBEM method due to the involvement of the double integrals. Without doubt, these properties make the proposed SGBEM method more convenient for non-smooth boundary problems from the view point of numerical implementation.

(ii) Scattering of pressure field around a cube

The acoustic scattering of plane waves with unit amplitude (e^{-ikx}) at normal incidence on a rigid cube with length a (a= 1) is considered to check the practicality of the present method for non-smooth boundaries. The cube is rotated so that the plane waves are toward its corner.

For comparison purposes, 3 different-sized models are

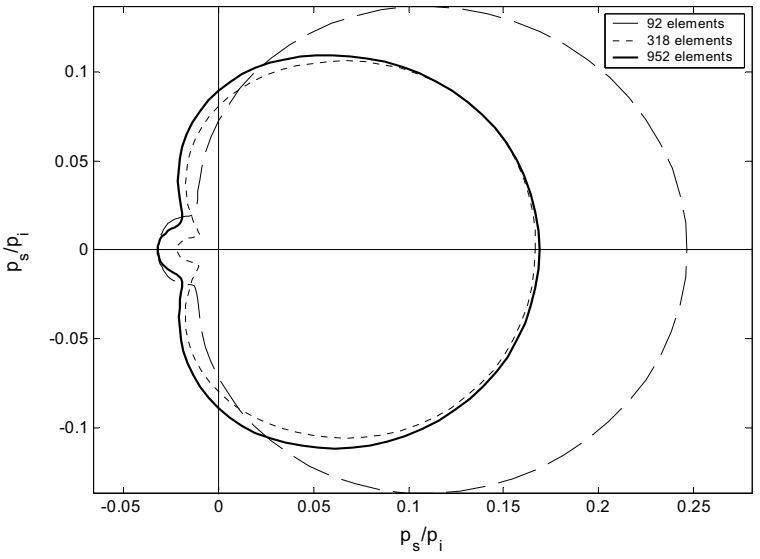

(a)

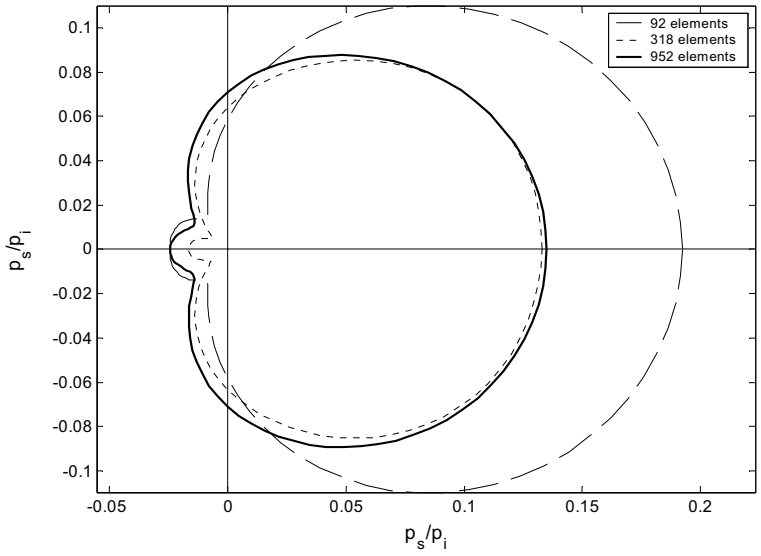

(b)

Figure 13 : The angular dependence of $\frac{p_s}{p_i}$ for a truncated ordinary cone with (a) $r = 8.0$; (b) $r = 10.0$; and $ka = 1$

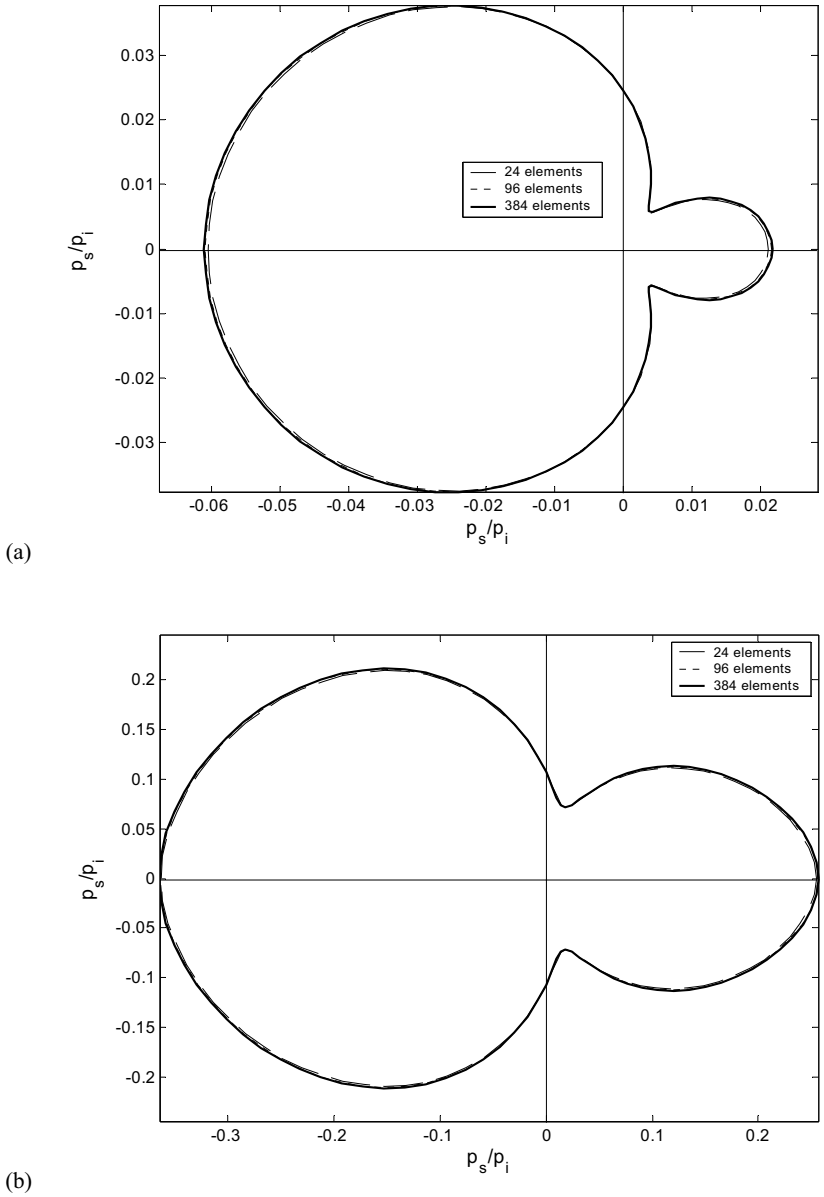

Figure 14 : The angular dependence of $\frac{p_s}{p_i}$ for a cube with (a) $r = 1.0$; (b) $r = 5.0$; and $ka = 1$

used for ka = 1 (24 elements; 96 elements; 384 elements). The analytical solution for the above problem is unavailable and hence the solution at the horizontal plane of symmetry, which is aligned with the incoming wave, is studied. The non-dimensionalized scattered pressure p_s/p_i, at distance r from the center of the cube, versus the polar angle is plotted in Fig. 14 for non-dimensionalized wave number ka = 1.0. The solution shows that the method converges, as the number of elements increases.

5 Conclusion

The symmetric Galerkin Boundary Element formulations of the regularized forms of newly derived non-hyper-singular boundary integral equations [denoted in the paper as "SGBEM-R-ϕ-BIE" and "SGBEM-R-q-BIE"] have been presented, in order to overcome the difficulties with hyper-singular integrals involved in the composite Helmholtz integral equations presented by Burton and Miller [Burton and Miller (1971)]. The methods based on BEM-R-ϕ-BIE, and BEM-R-q-BIE, using direct collocations of (36), is presented elsewhere [Qian, Han, and Atluri (2003)]. The weak singularities make the present approach highly accurate and more efficient in the numerical implementation. Also the non-uniqueness problem is resolved with the demonstration of the example of a pulsating sphere, i.e., the approach is applicable even at the characteristic frequencies. Moreover, there is no requirement of smoothness of the chosen trial functions for ϕ and q, and C^0 continuity is sufficient for numerical implementation. Another advantage of symmetric Galerkin formulation is the symmetry of system matrix. Further investigation will extend the present approach, using the Meshless Local Petrov Galerkin approach, to develop MLPG-R-ϕ-BIE, and MLPG-R-q-BIE, respectively. These MLPG methods will be presented in subsequent papers.

Acknowledgement: This work was supported by the Army Research Laboratory, in a collaborative research agreement with the University of California, Irvine. Sincere thanks are expressed to Drs. R.Namburu, A.M. Rajendran, for their keen interest and helpful suggestions.

References

Aimi, A.; Diligenti, M.; Lunardini, F.; Salvadori, A. (2003): A new approach of the panel clustering method for 3D SGBEM. *CMES: Computer Modeling in Engineering & Sciences* 4(1): 31-49.

Andra, H. (1998): Integration of singular integrals for the Galerkin-type boundary element method in 3D elasticity. *Comp. Methods Appl. Mech. Engng* 157: 239-249.

Atluri, S. N. (1985): Computational solid mechanics (finite elements and boundary elements) present status and future directions, *The Chinese Journal of Mechanics*.

Atluri, S. N.; Han, Z. D.; Shen, S. (2003): Meshless Local Patrov-Galerkin (MLPG) approaches for weakly-singular traction & displacement boundary integral equations, *CMES: Computer Modeling in Engineering & Sciences* 4(5): 507-516.

Atluri, S. N.; Shen, S. (2002a): *The meshless local Petrov-Galerkin (MLPG) method*. Tech. Science Press, 440 pages.

Atluri, S. N.; Shen, S. (2002b): The meshless local Petrov-Galerkin (MLPG) method: A simple & less-costly alternative to the finite element and boundary element method. *CMES: Computer Modeling in Engineering & Sciences* 3(1): 11-52.

Breuer, J.; Steinbach, O.; Wendland, W.L. (2002): A wavelet boundary element method for the symmetric boundary integral formulation. *IABEM 2002, International Association for Boundary Element Methods,* UT Austin, TX, USA, May 28-30.

Burton, A.J., Miller, G.F. (1971): The application of the integral equation method to the numerical solution of some exterior boundary value problems. *Proc. R. Soc. London Ser. A* 323: 201-210.

Chen, Z.S.; Hofstetter, G.; Mang, H.A. (1997): A symmetric Galerkin formulation of the boundary element method for acoustic radiation and scattering. *J. Comp. Acoust.* 5(2): 219-241.

Chien, C.C.; Rajiyah, H.; Atluri, S.N. (1990): An effective method for solving the hypersingular integral equations in 3-D acoustics. *J. Acoust. Soc. Am.* 88(2): 918-937.

Erichsen, S.; Sauter, S.A. (1998): Efficient automatic quadrature in 3-d Galerkin BEM. *Com. Methods Appl. Mech. Engng* 157: 215-224.

Gray, L.J.; Paulino, G.H. (1997): Symmetric Galerkin boundary integral formulation for interface and multi-zone problems. *Int. J. Numer. Meth. Eng.* 40: 3085-

3101.

Han. Z.D.; Atluri, S. N. (2002): SGBEM (for Cracked Local Subdomain) – FEM (for uncracked global Structure) Alternating Method for Analyzing 3D Surface Cracks and Their Fatigue-Growth. *CMES: Computer Modeling in Engineering & Sciences* 3(6): 699-716.

Han, Z.D.; Atluri, S.N. (2003a): On simple formulations of weakly-singular tBIE&dBIE, and Petrov-Galerkin approaches, *CMES: Computer Modeling in Engineering & Sciences* 4(1): 5-20.

Han. Z.D.; Atluri, S. N. (2003b): Truly Meshless Local Patrov-Galerkin (MLPG) solutions of traction & displacement BIEs. *CMES: Computer Modeling in Engineering & Sciences* 4(6): 665-678.

Hwang, W.S. (1997): Hyper-singular boundary integral equations for exterior acoustic problems. *J. Acoust. Soc. Am.* 101: 3336-3342.

Meyer, W.L.; Bell, W.A.; Zinn, B.T.; Stallybrass, M.P. (1978): Boundary integral solutions of three dimensional acoustic radiation problems, *Journal of Sound and Vibration* 59(2): 245-262.

Nikishkov, G.P.; Park, J.H.; Atluri, S.N. (2001): SGBEM-FEM alternating method for analyzing 3D nonplanar cracks and their growth in structural components, *CMES: Computer Modeling in Engineering & Sciences* 2(3): 401-422.

Okada, H.; Atluri, S. N. (1994): Recent developments in the field-boundary element method for finite/small strain elastoplasticity, *Int. J. Solids Struct.* 31(12-13): 1737-1775.

Okada, H.; Rajiyah, H.; Atluri, S. N. (1989a): A Novel Displacement Gradient Boundary Element Method for Elastic Stress Analysis with High Accuracy, *J. Applied Mech.* April: 1-9.

Okada, H.; Rajiyah, H.; Atluri, S. N. (1989b): Non-hypersingular integral representations for velocity (displacement) gradients in elastic/plastic solids (small or finite deformations), *Comp. Mech.* 4: 165-175.

Okada, H.; Rajiyah, H.; Atluri, S. N. (1990): A full tangent stiffness field-boundary-element formulation for geometric and material non-linear problems of solid mechanics, *Int. J. Numer. Meth. Eng.* 29(1): 15-35.

Qian, Z.Y.; Han, Z.D.; Atluri, S.N. (2004): Non-Hyper-Singular Integral Equations for Acoustic Problems, with Direct Collocation Implementation. (to appear)

Reut, Z. (1985): On the pboundary integral methods for the exterior acoustic problem. *J. Sound and Vib.* 103: 297-298.

Schenck, H.A. (1968): Improved integral formulation for acoustic radiation problems. *J. Acoust. Soc. Am.* 44: 41-58.

Terai, T. (1980): On calculation of sound fields around three dimensional objects by integral equation methods. *J. Sound Vib.* 69: 71-100.

Wu, T.W.; Seybert, A.F.; Wan, G.C. (1991): On the numerical implementation of a Cauchy principal value integral to insure a unique solution for acoustic radiation and scattering. *J. Acoust. Soc. Am.* 90: 554-560.

Yan, Z.Y.; Hung, K.C.; Zheng, H. (2003): Solving the hypersingular boundary integral equation in three-dimensional acoustics using a regularization relationship, *J. Acoust. Soc. Am.* 113(5): 2674-2683.

Yang, S.A. (2000): An investigation into integral equation methods involving nearly singular kernels for acoustic scattering. *J. Sound Vib.* 234(2): 225-239.

Zhang, J.M.; Yao, Z.H. (2001): Meshless regular hybrid boundary node method. *CMES: Computer Modeling in Engineering & Sciences* 2(3): 307-318.